Soils and Rocks
An International Journal of Geotechnical and Geoenvironmental Engineering
www.soilsandrocks.com
ISSN 1980-9743
ISSN-e 2675-5475

Assessment of potential of Algerian iron ore tailing as a standalone stabilizing material for expansive clayey soils

Rima Tobal[1#], Zied Benghazi[1], Adel Djellali[1], Debojit Sarker[2]

Article

Keywords
Expansive soils
Iron ore tailings
Soil stabilization
Environmental soil engineering
Sustainable geotechnics

Abstract

Expansive soils (ES) are prevalent in semi-arid regions, notably in North African countries. Such soils pose significant infrastructure challenges due to their shrink-swell behavior upon moisture variation. Stabilizing ES using tailings offers a dual benefit: enhancing soil properties and addressing tailing disposal concerns. Reusing and recycling mine tailing materials in problematic earthwork applications, such as ES, could mitigate environmental pollution due to mining activities and protect natural resources. This work is the first study to demonstrate the pozzolanic reactivity and mechanical benefits of finely ground Algerian iron ore tailing (IOT) as a standalone stabilizing agent for ES. Soil samples were treated with varying IOT concentrations (8%, 10%, and 12%) and subjected to a series of tests, including sieve analysis, X-ray fluorescence (XRF), scanning electron microscope (SEM), and X-ray diffraction (XRD). Geotechnical properties were assessed through standard Proctor compaction, unconfined compression strength (*UCS*), free swell, oedometer, and shear strength tests over different curing periods. Results show that the IOT effectively reduces ES expansion and improves the properties by decreasing plasticity index (*PI*), free swell index (*FSI*), swelling pressure (*Sp*), and maximum dry density (*MDD*), as well as increasing optimum moisture content (*OMC*), cohesion (*C*), frictional angle (ϕ) and *pH*. The mixture with 12% IOT demonstrated the highest improvement in compressive strength, highlighting its efficiency in stabilizing ES. This research proves the ability of IOT as a sustainable stabilizer for ES. It gives a second use to tailing material in geotechnical projects.

1. Introduction

Expansive soils (ES) are prevalent worldwide. They are typically found in semi-arid regions of tropical and temperate climatic zones and are common where yearly evaporation exceeds the precipitation (Plait, 1953). It is characterized by its high plasticity and high shrink-swell behavior due to the high percentages of its fine-grained clay mineral content, such as montmorillonite, smectite, and illite minerals, which originate from aluminosilicate resources (Ikeagwuani & Nwonu, 2019; Khalifa et al., 2020; Randhawa & Chauhan, 2022). When the moisture is changed, there is a significant volumetric change, which negatively affects the engineering properties of the upper layer in the active zone of these soils (Ferreira et al., 2013; Nelson et al., 2015). The changes in the soil volumes are also influenced by factors such as the stress history, soil's structural arrangement, specific area, and mineralogical particle interaction (Sakr et al., 2024). The financial impact of ES contributes to billions of dollars in losses annually, leading to a dramatic rise in insurance claims (Driscoll & Crilly, 2000; Devkota et al., 2022).

Identifying cost-effective remedial measures to improve soil for safe application in engineering and hydraulic projects, including earth dams, embankments, retaining walls, and pavements (Yu et al., 2014; Ijaz et al., 2020; Ikeagwuani, 2021; Zimar et al., 2022). Lime, cement, and bitumen are common stabilizers for soils (Roshan & Rashid, 2024). Meanwhile, ongoing research investigates the feasibility of utilizing waste materials and their environmental compatibility. Such efforts advance sustainable geotechnical engineering by promoting the beneficial reuse of oxides present in various industrial waste products (Osinubi et al., 2015). Other recent works have evaluated alternative stabilizers and innovative mixtures in expansive or problematic soils (Ocheme et al., 2023; Ahmadi et al., 2024; Paiyz et al., 2025, Sagidullina et al., 2025), highlighting the growing trend toward sustainable and non-traditional binders.

[#]Corresponding author. E-mail address: rima.tobal@univ-tebessa.dz
[1]Echahid Larbi Tebessi University, Mining Institute, Department of Mining and Geotechnology, Tebessa, Algeria.
[2]HNTB, Parsippany, NJ, USA.

Submitted on May 9, 2025; Final Acceptance on September 18, 2025; Discussion open until May 31, 2026.
Editor: Renato P. Cunha
https://doi.org/10.28927/SR.2026.007825

Iron ore tailings (IOT) are a byproduct of iron ore mining, generated in substantial quantities, with approximately two tons of tailings produced per ton of ore extracted (Adepoju & Olaleye, 2001; Ajaka, 2009; Moran-Palacios et al., 2019). Improper disposal of IOT results in significant ecological harm, including soil and water contamination and dam failures, as documented in Brazil (Etim et al., 2017; Moran-Palacios et al., 2019; Sá et al., 2022). The mineralogical similarity of IOT to parent ores imparts considerable chemical potential for reuse in construction applications. Recycling IOT offers several environmental and economic advantages, such as reducing the carbon footprint, conserving natural resources, and providing a cost-effective construction material (Benghazi et al., 2024).

Several studies have used IOT in soil stabilization. Jaharou (2015) and Etim et al. (2017) combined IOT with lime to improve ES strength for road construction. While Tong et al. (2021) achieved significant mechanical gains by using IOT with cement. Osinubi et al. (2015) reduced cement consumption by partially replacing it with IOT. Other studies investigated IOT sand as a partial soil replacement (Chu et al., 2021; Chethan et al., 2022), reporting improvements in density and swelling reduction but modest chemical reactivity.

These studies specifically combine iron ore tailings (IOT) with lime or cement, which increases both project costs and carbon emissions. The research predominantly examined coarse IOT fractions, leading to mainly physical stabilization effects. The pozzolanic reactivity of finely ground Algerian IOT has not been systematically investigated, and there is no evidence confirming its compliance with Class C pozzolan standards or its ability to induce cementitious bonding independently. Additionally, few studies have combined mechanical testing with scanning electron microscopy (SEM) and X-ray diffraction (XRD) analyses to directly correlate microstructural changes with strength improvements in binder-free IOT stabilization.

The present work addresses this research gap by evaluating the pozzolanic reactivity and mechanical properties of finely ground Algerian IOT to binder-like fineness as a potential standalone stabilizing agent for ES with a low carbon footprint. The IOT used in this study meets ASTM criteria for Class C pozzolans, making it a viable substitute for traditional binders from both environmental and technical perspectives. Therefore, different percentages (8, 10, and 12%) of IOT relative to the dry weight of the ES were studied. Sieve analysis, X-ray fluorescence (XRF), SEM, and XRD were used to identify the properties of ES, IOT, and the treated soil mixtures. Samples compacted at the optimum moisture content (*OMC*) using the standard Proctor compaction test according to the ASTM standards were subjected to *UCS*, free swell, oedometer, and shear strength tests. The findings reveal that IOT addition reduces plasticity, swelling potential, and compressibility while enhancing strength and stiffness. Microstructural analysis confirms the formation of pozzolanic reaction products, including calcium silicate hydrates (C-S-H) and ettringite, which contribute to the observed improvements. The optimal performance was observed at 12% IOT content.

This work highlights the environmental and engineering viability of using Algerian IOT as a sustainable, standalone stabilizer for ES, offering a dual benefit of reducing mining waste and minimizing carbon-intensive binder use in geotechnical applications.

2. Materials and methods

2.1 Study area and materials

The ES used in this study was collected from Doukkane, near Tebessa city in eastern Algeria (Figure 1), a semi-arid region with average annual rainfall between 250-300 mm (Zereg et al., 2018). The subsoil is dominated by clayey marls of Plio-Quaternary origin (Djellali et al., 2022). The IOT was sourced from the Boukhadra mine, located in the same region.

The representative samples of both materials were prepared in the laboratory using the coning and quartering methods. The ES used in the experiments was dried in the oven at 60 °C to avoid the decomposition of specific soil components, which may affect the accuracy of subsequent soil analyses (ASTM, 2017a).

The IOT was first passed on the crushing and grinding machine and then sieved until a powder with fineness close to that of conventional stabilizing binders with over 95% of particles smaller than 45µ to enable the IOT to better adhere to the ES (Wu et al., 2022). The physical properties and the chemical composition of the used materials are illustrated in Tables 1 and 2.

Based on the PSD curve presented in Figure 2 and the ASTM D2487-17 standard (ASTM, 2017c), the uniformity and curvature coefficients (*Cu*) and (*Cc*) were calculated as 11.11 and 1.07 for ES, 4.33 and 1.26 for IOT (Table 2), which indicates that both materials exhibit well-graded characteristics. Figure 2 shows that the ES is composed of 75,17% fine particles passing the No. 200 sieve (75 µm), including 24% of clay. The $CaCO_3$ content in the Doukkane soil exceeds 35%, indicating that it has a marly nature (Foucault et al., 2020). According to Atterberg's limits (Table 1) and the Unified Soil Classification system (USCS) (ASTM, 2017c), Doukkane's soil is classified as high plastic clayey marl with significant activity and a high swelling potential according to Dakshanamurthy & Raman (1973) and Chen (1988) classifications. The ground IOT is brownish-red in color and has high iron oxide content with very low carbonate (Table 2). According to ASTM C618-23 (ASTM, 2019a) standard, the ground IOT is qualified as class C Pozzolan, suitable for use as a supplementary cementitious material.

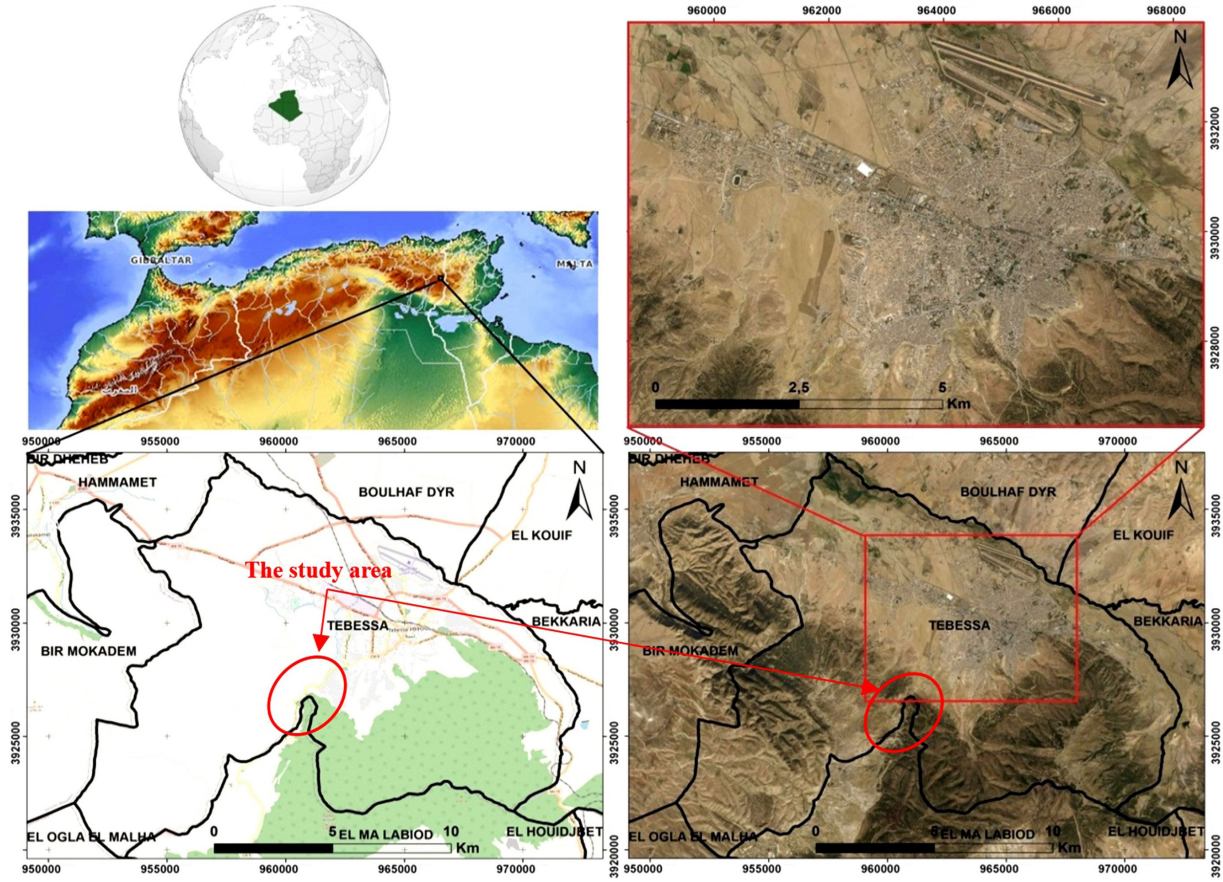

Figure 1. Position of the study zone in eastern part of Algeria (Djellali et al., 2022).

Table 1. Physical properties of used materials.

Properties	ES	IOT
Uniformity coefficient C_U=(D_{60}/D_{10})	11.11	4.33
Coefficient of curvature C_C = (D_{30})^2/ (D_{10} x D_{60})	1.07	1.26
Unit Weight, γ_s (kN/m^3)	25.21	39.47
Specific Gravity, G_s	2.52	3.95
Natural moisture (%)	21.23	-
pH	7.51	8.60
MBV	6.67	0.33
Ac	1.74	-
Swelling pressure, *SP* (kPa)	260	-
Free swell index, *FSI* (%)	15	-
Liquid limit, *LL* (%)	54	20
Plastic limit, *PL* (%)	21	17
Shrinkage limit, *SL* (%)	14.71	18.57
Plasticity index, *PI* (%)	33	3
Maximum Dry Density, *MDD* (kg/m^3)	1770	-
Optimum Moisture Content, *OMC* (%)	18	-

Table 2. Chemical properties of ES and IOT using XRF analysis.

Material	SiO_2	Al_2O_3	Fe_2O_3	CaO	MgO	K_2O	SO_3	SrO	P_2O_5	Na_2O	TiO_2	Cl	As_2O_3	MnO	SrO	BaO	*LOI*
ES (%)	35.9	15.9	8.78	26.4	1.74	1.65	7.32	0.189	0.159	0.31	1.93	0.075	-	-	-	-	8.029
IOT (%)	20.01	6.00	43.16	2.54	0.39	0.28	1.33	0.155	0.087	-	-	-	0.032	3.01	0.155	2.61	2.422

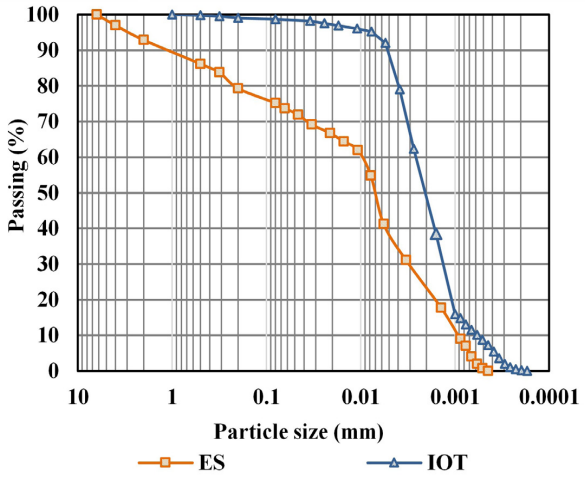

Figure 2. Particle size distribution curves of ES and IOT.

2.2 Experimental methods

Three mixtures were prepared by adding 8%, 10%, and 12% of the ground IOT to the ES. This range was selected based on previous studies showing optimal performance with 5-15% industrial byproduct addition (Etim et al., 2017; Sani et al., 2019; Chethan et al., 2022) and preliminary trials indicating that >12% increased water demand and reduced compaction, while <8% gave marginal gains.

A series of tests was conducted to evaluate the geotechnical properties of treated soil, including *OMC* and *MDD*, *FSI* and *Sp*, compression (C_c) and swelling (C_s) coefficients, *UCS* and Young's modulus (*E*), frictional angle (ϕ), and cohesion (*C*). All these properties were determined according to the American Society for Testing and Materials (ASTM) standards. The chemical and mineralogical components of the studied mixtures were identified using SEM and XRD.

2.2.1 Geotechnical testing

The following laboratory tests were conducted on untreated and treated samples:

- Atterberg Limits (ASTM, 2018): To determine liquid limit (*LL*), plastic limit (*PL*), and plasticity index (*PI*);
- Shrinkage Characteristics (ASTM, 2008): Shrinkage limit (*SL*), linear shrinkage (*Ls*), and shrinkage index (*Is*);
- Methylene Blue Value (*MBV*) test (ASTM, 2020): To assess the presence of clay minerals in soils;
- *pH* test (ASTM, 2019b): To evaluate the alkalinity or acidity of the studied materials;
- Proctor compaction test (ASTM, 2021): To determine *OMC* and *MDD* of the studied mixtures;
- Free Swell and Swelling Pressure tests (ASTM, 2010): To evaluate the swelling potential and swelling pressure of soils when they are exposed to moisture, using oedometer cells under saturated conditions;
- One-Dimensional Consolidation test (ASTM, 2011): To assess the consolidation properties of the different prepared soil mixtures and obtain the compression index (C_c) and swelling index (C_s). The specimens were compacted at *OMC* to the target *MDD*, trimmed to fit the rigid rings, and placed in the oedometer cell with porous stones and filter papers at both ends. They were fully saturated before loading;
- Unconfined Compressive Strength (*UCS*) (ASTM, 2017b): Performed after curing for 2, 7, 14, and 28 days at a relative humidity exceeding 95% and a temperature of 20±1 °C. The molding of the samples was carried out in a mold with a diameter/height ratio of 1:2 (d=50.0 mm and h=100.0 mm). The compaction was conducted in 3 layers using a hydraulic press at a compaction load of 50 kN until the target *MDD* was reached, corresponding to the *OMC* for the different mixtures (Degirmenci et al., 2007), with a tolerance of ≤ 5% (Al-Obaidi et al., 2020);
- Direct Shear Test (DST) (ASTM, 2017d): To determine shear strength parameters: *C* and ϕ. The specimens were compacted at the *OMC* to the target *MDD*, cut to fit the shear box, leveled flush with the surface, and sheared with a strain rate of 1.2mm/min, without water drainage.

2.2.2 Microstructural analysis

- Scanning Electron Microscopy (SEM): Conducted at 5,000× magnification to observe morphological changes due to IOT addition;
- X-ray Diffraction (XRD): Performed to identify mineralogical phases and confirm the formation of pozzolanic hydration products. Patterns were recorded after drying and grinding samples to <75 µm. Peak positions and intensities provided insight into phase transformations and crystallinity. Analysis was conducted using Match! 4 Software.

3. Results and discussion

3.1 Effect of IOT on the Atterberg limit and activity index

The untreated ES exhibited high plasticity with an *LL* of 54.08%, *PL* of 21.11%, and *PI* of 32.97%, classifying it as high-plastic clay (CH) under USCS. In contrast, the IOT had much lower plasticity (*PI* = 3.19%). The inclusion of IOT resulted in a consistent decrease in *PI* across all mixtures, with the 12% IOT blend showing the most significant reduction. This is attributed to the dilution of expansive clay minerals, particularly montmorillonite, and the replacement of exchangeable cations by iron-rich species from IOT. Cation exchange and pozzolanic reactions between reactive silica/alumina in IOT and the clay minerals likely contributed

to flocculation and agglomeration, reducing plasticity and improving workability. These findings align with those of Sani et al. (2019), Etim et al. (2022), and Regasa et al. (2023), who observed similar trends using industrial byproducts. The decrease in *PI* value implies a decrease in the soil's expansion potential (Jayasree et al., 2015).

From Figure 3, the intersection point *PI* versus *LL* is closer to the U-line, which indicates that it contains a significant amount of active clay minerals predominated by illite with the presence of montmorillonite. The activity of clay (*Ac*) is calculated using Equation 1 (Seed et al., 1962):

$$Ac = \frac{PI}{c-5} \quad (1)$$

where: *PI*: plasticity index (%); *c*: percentages of particles finer than 2μm (%).

The activity result of the ES (1.74) is above the threshold value of 1.25. According to Skempton. (1953), the ES is classified as active soil, and the active minerals of this clay are illite Na+ and montmorillonite Ca^{2+}.

The *SL* (Budhu, 2011), the linear shrinkage (*Ls*) (Altmeyer, 1955), and the shrinkage index (*Is*) (Jayasree et al., 2015), were calculated according to Equations 2, 3 and 4, respectively:

$$SL = 46.4\frac{(LL+45.5)}{(PI+46.4)} - 43.5 \quad (2)$$

$$Ls = PI / 2.13 \quad (3)$$

$$Is = LL - SL \quad (4)$$

The calculated values depict that the *SL* and *Ls* are inversely proportional (Table 3). The *SL* increases with the decrease of *Ls* and *Is*, which indicates the soil's capacity to resist the volume change on desiccation (Jayasree et al., 2015). According to the Indian Standard Classification (IS, 1987), the degree of severity for the ES and IOT is critical and non-critical, respectively. The addition of IOT as a stabilizer material decreases the mixtures' expansion severity to marginal, as evidenced by the soil treated with 12% IOT.

3.2 Effect of IOT on methylene blue value and *pH*

Figure 4 shows the influence of IOT content on the methylene blue value (*MBV*) and *pH*. The *MBV* reflects the clay activity and swelling potential, while *pH* indicates the alkalinity necessary to activate pozzolanic reactions.

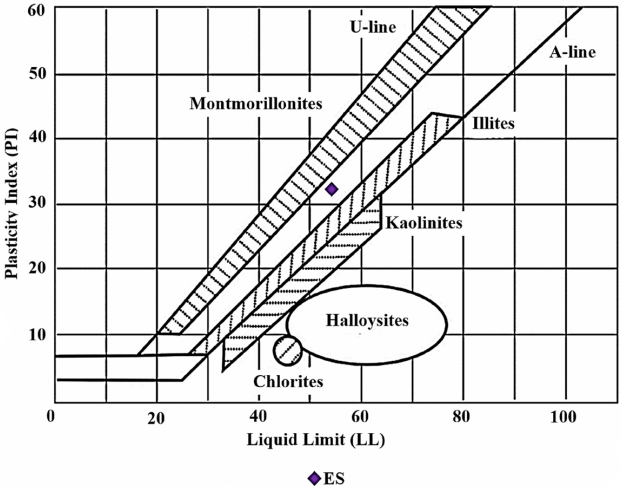

Figure 3. Determination of the clay minerals in the studied ES based on Casagrande's plasticity chart (Constantinescu & Constantinescu, 2011).

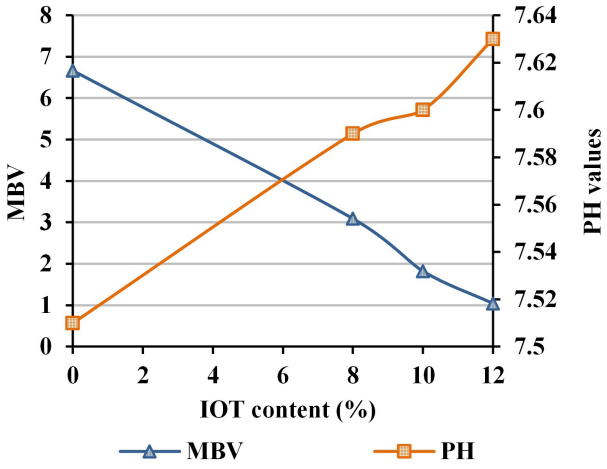

Figure 4. Effect of IOT content on *MBV* and *pH* values.

Table 3. Shrinkage factors values of the ES, IOT, and stabilized soil.

	SL	*Ls*	*Is*
0%	14.71	15.48	39.37
8%	19.35	11.88	32.27
10%	19.86	11.46	31.35
12%	29.81	6.75	20.70
IOT	18.57	1.50	2.27

Based on Magnan & Youssefian (1989), the ES is classified as very active with an *MBV* of 6.67. *MBV* decreased progressively with higher IOT content, reaching 1.04 at 12% IOT, indicating reduced swelling potential and texture modification (Yukselen & Kaya, 2008; Chassagneux et al., 1996). These results indicate that fine, silica-rich IOT can effectively temper clay surface reactivity and re-texture the fabric—mechanisms analogous to those reported for other wastes but with lower carbon intensity (Zimar et al., 2022, 2024).

The *pH* values increased slightly from 7.51 to 7.63 with IOT addition, attributed to its intrinsic alkalinity (*pH* 8.60). According to Vogel & Kasper (2002) and Etim et al. (2017), such *pH* elevation reduces soil contaminants' solubility and promotes stability. The *pH* rise enhances pozzolanic reactions and cation exchange, contributing to the formation of cementitious products, which contribute to the enhancement of interparticle bonds and, consequently, the mechanical strength of treated soil (Abbey et al., 2021).

3.3 Effect of IOT on the compaction characteristics

The Standard Proctor test results (Figure 5) reveal that the *OMC* increased from 18% to 20% with IOT addition, while *MDD* decreased from 1770 to 1660 kg/m³. The increase in *OMC* is likely due to the higher surface area of ground IOT, which demands more water for lubrication and hydration reactions. Conversely, the lower *MDD* results from the relatively lower specific gravity and packing efficiency of the treated mixtures due to agglomeration of particles (Turan et al., 2022). These observations are in line with results reported by Sharma et al. (2018), Ikeagwuani & Nwonu (2019), and Spagnoli & Shimobe (2020), as well as the consensus in the literature. This can be attributed to the increase in the required amount of water for lubricating the soil-IOT mixtures, which have a larger specific surface area (Waleed & Alshawmar, 2025). Additionally, the hydration reactions between the IOT and the cations of the ES particles consumed a part of the necessary water amount for the treated soil densification (Ikeagwuani & Nwonu, 2019; Etim et al., 2017).

3.4 Effect of IOT on the *FSI* and the swelling pressure

Figure 6 illustrates the variation of *FSI* and *Sp* as a function of IOT content obtained from the free swell test. Both *FSI* and *Sp* decreased significantly by 72% and 71.5%, respectively, at 12% IOT content, as compared to the ES. This reduction can be attributed to the modification of the soil structure through the consumption of water in IOT-soil hydration reactions, leading to a decrease in swelling ability (Etim et al., 2017). Similar behavior was reported when using industrial and agro-wastes along with alkaline binders like lime, such as fly ash (Sambre et al., 2024), waste paper sludge (Tanyildizi et al., 2024), and rice husk ash (Rahaja et al., 2024). The results revealed that the finely ground IOT, acting alone, is able to reduce the swelling potential of ES.

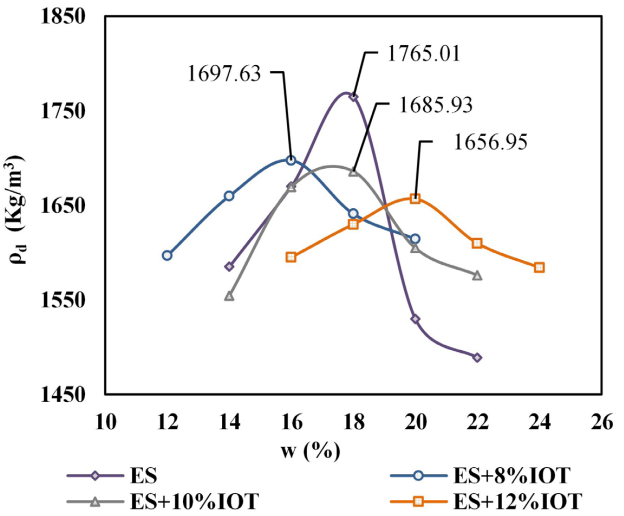

Figure 5. Variation of *ρd* and *OMC* values of ES and different mixtures.

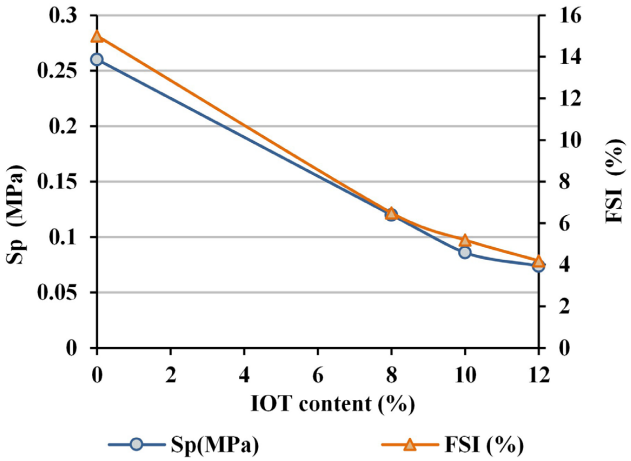

Figure 6. Variation of *FSI* and *Sp* for different mixtures of soil-IOT.

3.5 Effect of IOT on the consolidation behavior

The void ratio (*e*) versus log effective stress curves (Figure 7) show that treated soils exhibit a steeper compression path at moderate IOT contents (8-10%), indicating denser packing and void filling. At 12% IOT, the soil-IOT mixture exhibited a higher *e* because the fine particles and larger surface area increased water demand, which reduced the achievable dry density during compaction. In addition, particle agglomeration due to hydration at this dosage modified the packing structure and created intergranular voids, making it stiffer for deformation, resulting in a rebound in *e* during consolidation (Tan et al., 2016; Aksu & Eskisar, 2023; Farenzena et al., 2024). This behavior is also noted in compression and particle-breakage studies of IOT, where fines, fabric change, and breakage control compressibility (Silva et al., 2024; Ji et al., 2025).

Compression index (C_c) slightly increased from 0.22 to 0.29, while swelling index (C_s) decreased significantly from 0.09 to 0.03 (Table 4). The increased compressibility may reflect structural reorganization due to pozzolanic reaction products, while reduced C_s indicates better resistance to re-expansion—an important factor for long-term stability. According to Tan et al. (2016), larger agglomerates from soil-IOT reactions destabilize the soil fabric, altering structure and pore distribution under equal compaction. However, the obtained C_c values fall within the range typically observed for medium-soft clayey soils with illite as the main clay mineral (Widodo & Ibrahim, 2012; Ye et al., 2015), indicating that the soil-IOT mixtures remain within the acceptable engineering limits of compressibility for clay soils (C_c=0.285 to 0.968) (Ibrahim et al., 2012).

3.6 Effect of IOT on the unconfined compressive strength and Young's modulus

Figure 8 presents the variation of *UCS* over the curing time of soil-IOT mixtures. It is observed that the addition of IOT increases the *UCS* of the treated soil proportionally and enhances its deformation, which leads to a notable 27% improvement in *UCS* values. The trend demonstrates the progressive development of pozzolanic bonds. The slight increase in *UCS* for the 12% OT-soil mixture, compared to other studied mixtures, results from the progressive formation of cementitious gels due to pozzolanic reactions, including C-S-H and C-A-H, as well as ettringite and iron-rich hydrates. These hydration products fill pores and enhance interparticle bonding and strength (Hossain & Mol, 2011; Etim et al., 2017; Kaze et al., 2021; Tang et al., 2024). Although the early strength development is comparatively lower than that observed in soils stabilized with cement, pozzolanic materials continue to develop mechanical strength beyond 28 days (Zeghichi & Benghazi, 2011).

A gradual increase in *UCS* and stiffness (E) was also observed in the untreated clayey marl during curing. This behavior can be attributed to the moisture redistribution under curing conditions leading to changes in suction, which effectively increase apparent strength and stiffness. The presence of natural $CaCO_3$ and active clay minerals in the marl may further contribute to mild self-cementation, explaining the observed strength gain even in the absence of IOT (Fukue et al., 1999).

Stress-strain curves (Figure 9) show a more brittle failure mode in treated soils, reflecting increased stiffness. The E values also rose with IOT content, peaking at 12% IOT (51.26 MPa), and slightly declining at 10% IOT (Figure 10). This suggests that 12% IOT yields the best stiffness-to-density balance, while further addition may lead to microstructural weakening due to over-agglomeration.

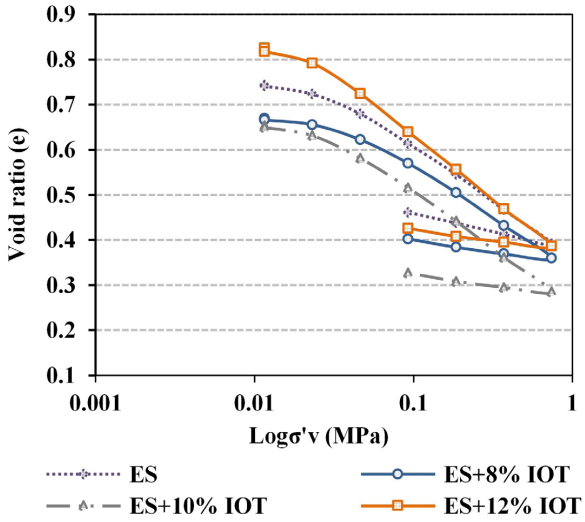

Figure 7. Variation of the *e* as a function of the vertical effective stress (log σ'v) for the different blends.

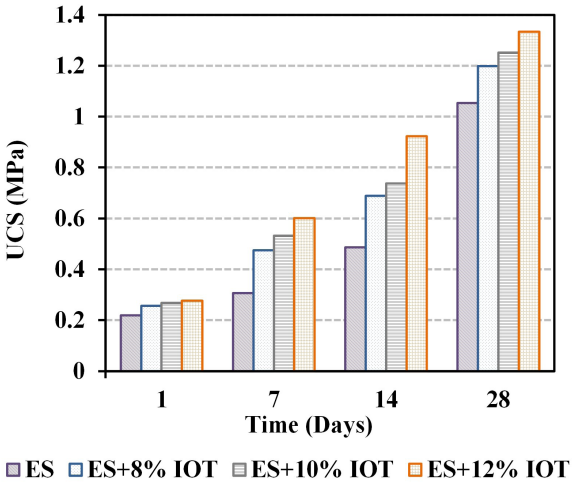

Figure 8. Variation of *UCS* at the curing time of soil-IOT mixtures.

Table 4. Deformation parameters of the different mixtures from the oedometer test.

	σ'_p (MPa)	C_c	C_s
ES	0.034	0.22	0.09
ES+8% IOT	0.060	0.23	0.06
ES+10% IOT	0.039	0.27	0.05
ES+12% IOT	0.028	0.29	0.03

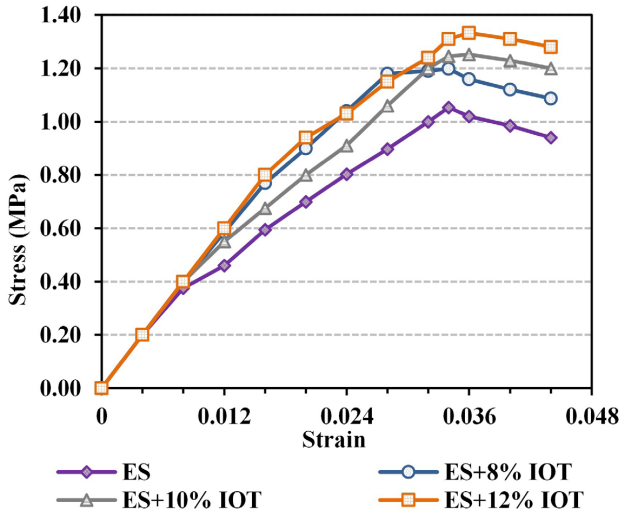

Figure 9. Variation of stress-strain of the soil-IOT mixtures.

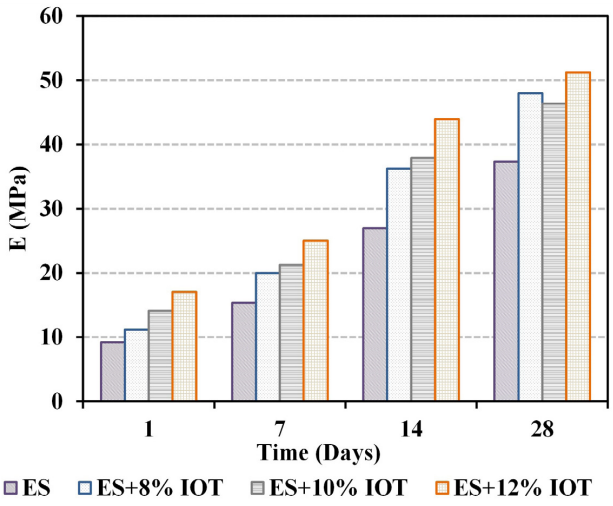

Figure 10. Variation of *E* for the soil-IOT mixtures.

The contribution of IOT in the improvement of the *E* modulus explains the increase in stiffness, which leads to a reduction in soil shrink-swell values (Adem & Vanapalli, 2014).

3.7 Effect of IOT on the shear strength parameters

Figure 11 illustrates the influence of IOT content on the *C* and the ϕ of the soil-IOT mixtures as determined by direct shear test. Notably, both *C* and ϕ display an increase of 46% and 56%, respectively, as the amount of IOT in the mixture reaches 12%. This rise can be attributed to the formation of C-S-H/C-A-H gel, which efficiently binds the IOT-soil particles together.

The observed increase in both *E* and *UCS* values is a result of the enhanced *C* of the treated soil (Hossain & Mol, 2011). According to Blayi et al. (2024), the fictional angle increases can be attributed to the flocculation effect of IOT on clay particles, making the mixture particles coarse. Additionally, the pozzolanic reactions induced by IOT influence the ϕ values through the formation of a higher quantity of large particle size fractions and, consequently, enhance the frictional forces within the mixture matrix (Petit et al., 2013; Farenzena et al., 2024).

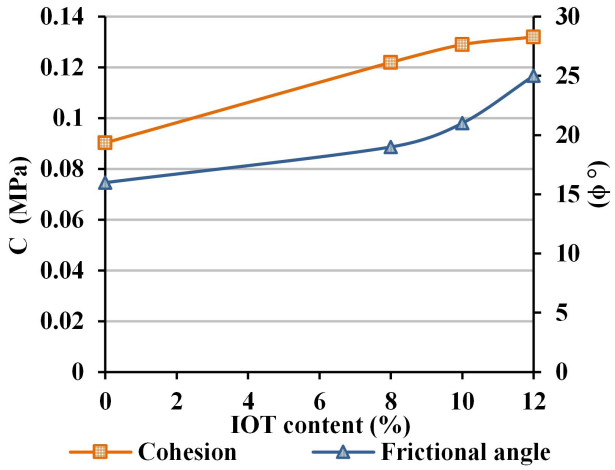

Figure 11. Effect of the IOT content on the *C* and friction angle.

3.8 Scanning electron microscopy results

Figure 12 presents SEM images of untreated ES, IOT, and soils stabilized with 8%, 10%, and 12% IOT at ×5000 magnification. The untreated ES (Figure 12a) exhibits a loose, porous structure with randomly oriented clay sheets (0.7-4 µm) and platy illite particles, contributing to high specific surface area (SSA) and swelling potential. In contrast, the IOT (Figure 12b) displays irregular granular particles (0.1-200 µm) with visible intergranular pores.

With IOT addition (Figures 12c-e), the microstructure becomes progressively denser as IOT fills voids and promotes particle bonding. Ettringite crystals—formed from reactions between soil sulphates and IOT aluminates—are clearly visible at 8% and 10% content, enhancing interparticle cohesion. At 12% IOT (Figure 12e), distinct C-S-H gel formation appears as bright regions, contributing to a cohesive matrix that improves strength. The presence of iron phosphate hydroxide and hematite further reduces porosity and adds rigidity to the stabilized soil structure.

3.9 X-ray diffraction results

The ES diffractogram (Figure 13a) revealed dominant illite (22.7%) and minor montmorillonite (0.8%), both responsible for high swelling due to interlayer water absorption. Calcite peaks indicated a marl composition, while gypsum, quartz, corundum, and minor goethite were also present.

Figure 13b shows IOT is mainly composed of hematite and quartz, with peaks at 32.9°, 33.2°, 35.6°, and 49.4° 2θ,

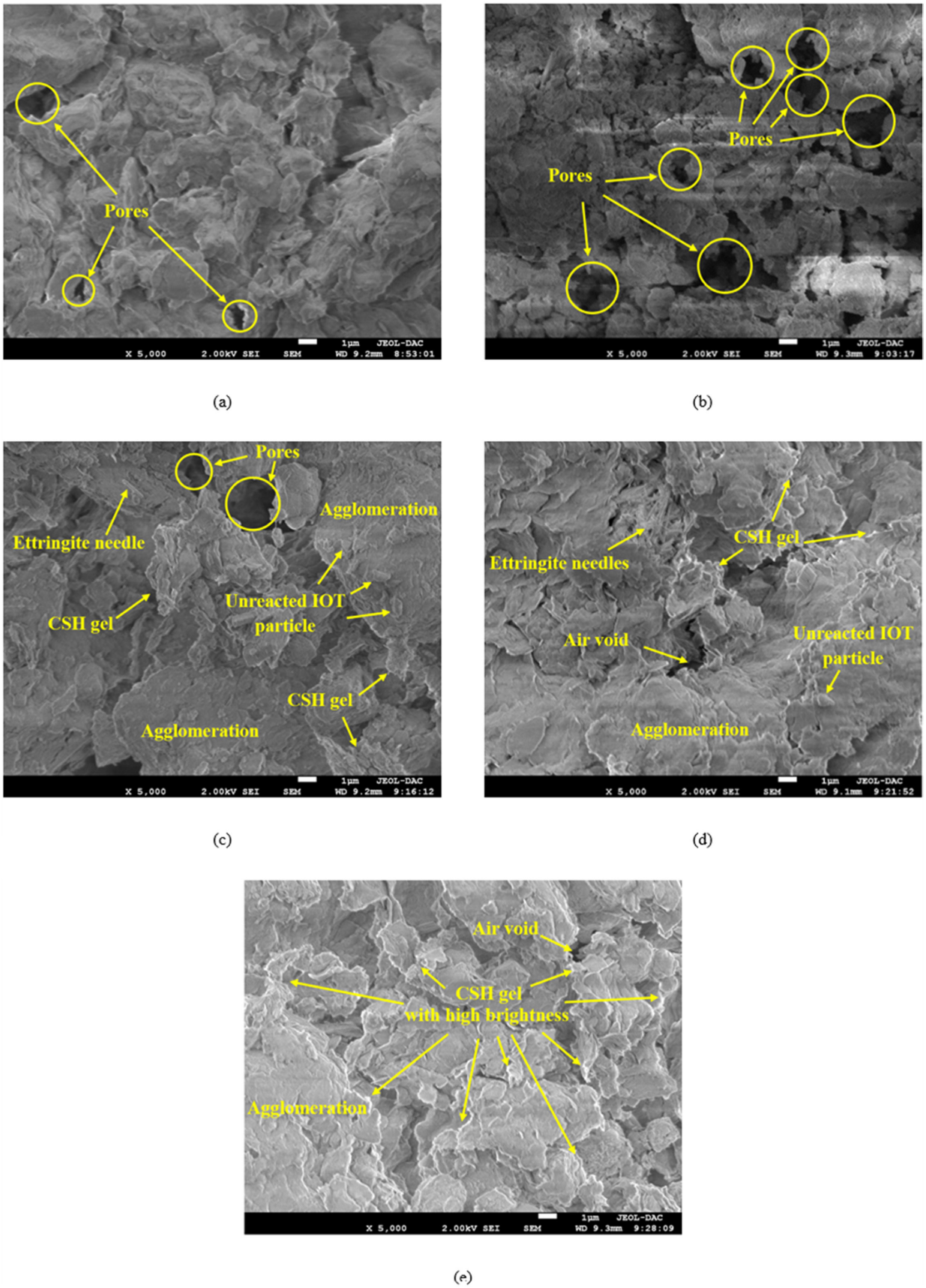

Figure 12. SEM images for: (a) ES; (b) IOT; (c) ES+8% IOT; (d) ES+10% IOT; (e) ES+12% IOT.

reflecting high residual iron. Secondary minerals include calcite, siderite, goethite, barytocalcite, and corundum, confirming the diverse iron-bearing mineralogy of IOT.

Figures 13c-e illustrates the mineralogical evolution of ES with IOT addition. Quartz remains stable, while illite and montmorillonite peak intensities decline, suggesting

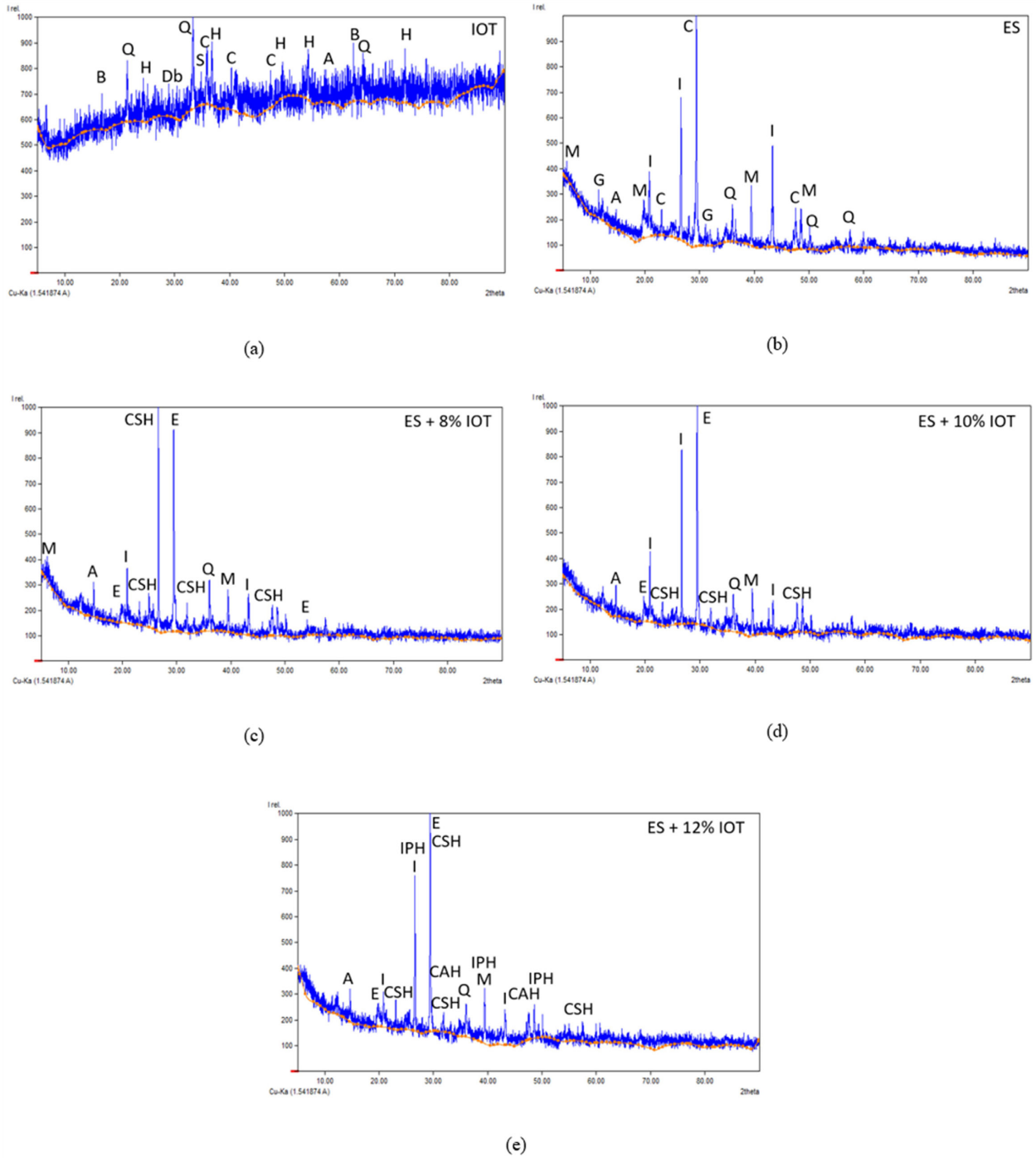

Figure 13. XRD analysis for: (a) ES; (b) IOT; (c) ES+8% IOT; (d) ES+10% IOT; (e) ES+12% IOT, where A: Corundum; B: Barytocalcite; C: Calcite; CAH: Katoite; CSH: Hillebrandite; Db: Dibarium hexairon oxide; E: Ettringite; G: Gypsum; H: Hematite; I: Illite; IPH: Iron phosphate hydroxide; M: Montmorillonite; Q: Quartz; S: Siderite.

reduced swelling potential. At 8% IOT, ettringite and C-S-H appear, indicating sulphate activation and pozzolanic activity. Higher IOT contents (10-12%) enhance ettringite formation and introduce hillebrandite (C-S-H), katoite (C-A-H), and iron phosphate hydroxide, as also observed in SEM.

These changes confirm that IOT promotes hydration reactions, forms cementitious products, and contributes to soil stabilization (Kaze et al., 2021; Tang et al., 2024), reducing expansiveness while enhancing mechanical integrity.

3.10 Qualitative sensitive analysis and limitations of the study

This research demonstrates the potential of binder-free Algerian IOT as a stabilizer for expansive clay. However, the study focuses on a specific expansive clayey soil, which may not represent the behavior of other expansive or marl-like soils worldwide. Although clayey marls are widespread, their mineralogical and chemical variability can result in different stabilization outcomes based on local soil characteristics.

Iron-ore tailings properties can vary substantially with ore type and processing route (mineralogy, fineness, *LOI*, sulphate content, free lime, and trace metal concentrations). These parameters control:

- The pozzolanic potential according to the ASTM C618-23 (ASTM, 2019a) specifications;
- Water demand and compactability;
- Likelihood of particle agglomeration;
- Possible leachable contaminants.

Qualitatively, tailings with higher reactivate silica/alumina and finer particle size are expected to increase pozzolanic bond formation and strength, whereas tailings with high sulphate, free carbonate, or organic/*LOI* content may modify reaction pathways (ettringite formation, carbonate buffering) and influence swelling or durability.

Therefore, when applying IOT-stabilization in other sites, we recommend a simple pre-screening protocol: (a) XRF to determine major oxides, (b) specific surface area of finely ground IOT, (c) *LOI* and free-carbonate content, and (d) a simple batch leach test for key contaminants.

Using those screens, engineers can qualitatively judge whether a given IOT source is likely to behave similarly to the Boukhadra IOT used in this study or whether additional treatment/activation or environmental control will be necessary.

This study focused on short-term laboratory performance of expansive soil treated with Algerian IOT (up to 28 days); long-term durability (wet-dry, freeze-thaw, sustained loading) and direct leaching behavior were not evaluated. However, pozzolanic materials are well known for their long-term hydration reaction leading to the enhancement of durability (Zeghichi & Benghazi, 2011).

According to El-Sharkawy et al. (2025), alkaline *pH* (7.5-8.0) and immobilization within low-solubility phases (iron oxides, C–S–H, and C–A–H) reduce metal mobility. A quantitative estimation of heavy and trace metals (As, Sr, Mn, Ba, Cu, Pb, Cr, Cd, and Hg) in ES-IOT mixtures, using Match! 4 software, shows that Pb level 426.9 ppm at 8% IOT, approaches or falls within the industrial thresholds according to Quebec Land Protection and Rehabilitation Regulation (Quebec, 2021) and the U.S. Environmental Protection Agency (2024). Other elements such as Cu, Mn, Ba, Sr, Cd, and Hg remained within acceptable regulatory ranges across all mixtures.

Nevertheless, standardized leaching tests such as TCLP (Toxicity Characteristic Leaching Procedure) or SPLP (Synthetic Precipitation Leaching Procedure) and field ageing trials remain necessary to confirm durability and ecological safety. Overall, findings indicate promising technical and environmental feasibility, but field validation is required before large-scale application.

4. Conclusion

The present study is the first to demonstrate the effective use of Algerian IOT, ground to pozzolanic fineness, as a standalone stabilizer for clayey ES without chemical binders. To assess its impact on ES geotechnical properties, an experimental program was conducted on untreated soil mixed with different IOT proportions.

The IOT-treated mixtures showed substantial reductions in plasticity index, free swell index, swelling pressure, and volumetric shrinkage, while C, ϕ, UCS, and E increased consistently with IOT content. These improvements are attributed to a combination of physical densification, resulting from the angular shape and fine grading of IOT particles, and chemical stabilization, driven by pozzolanic reactions with available CaO in the native clay matrix. The formation of cementitious compounds such as C-S-H and C-A-H gels was confirmed by SEM and XRD, explaining the observed strength gain and stiffness improvement.

Moreover, the rise in *pH* and decrease in *MBV* confirmed the flocculation and stabilization of clay particles, reflecting the interaction between the aluminosilicate phases in IOT and the active clay minerals. The reduced swelling potential further confirms the effectiveness of IOT in mitigating volume change issues associated with expansive soils.

The observed increase in *OMC* with the addition of IOT demonstrates that greater water input is necessary for compaction, which presents a potential limitation in field applications. Nevertheless, this requirement is counterbalanced by simultaneous enhancements in swelling reduction and mechanical strength.

Overall, the findings validate the potential of IOT as a cost-effective, low-carbon sustainable stabilizer. This approach supports the circular economy by valorizing mining waste while addressing critical geotechnical challenges. The conclusions may be extended to IOTs with similar oxide compositions and pozzolanic classes, making the approach relevant for broader engineering applications in regions facing both expansive soils and mine tailing disposal issues.

Declaration of interest

The authors declare that they have no conflicts of interest. All co-authors have observed and affirmed the contents of the paper and there is no financial interest to report.

Authors' contributions

Rima Tobal: conceptualization, data curation, visualization, writing – original draft, writing – review & editing. Zied Benghazi: conceptualization, data curation, methodology, supervision, validation, writing – original draft, writing – review & editing. Adel Djellali: conceptualization, methodology, supervision, project administration. Debojit Sarker: validation, writing – review & editing.

Data availability

All data produced or examined in the course of the current study are included in this article.

Declaration of use of generative artificial intelligence

This work was prepared with the assistance of generative artificial intelligence (GenAI) Chat GPT with the aim of enhancing the clarity of certain parts in the text. The entire process of using this tool was supervised, reviewed and when necessary edited by the authors. The authors assume full responsibility for the content of the publication that involved the aid of GenAI.

List of symbols and abbreviations

c	Percentages of particles finer than 2μm (%)
e	Void ratio
Ac	Activity of clay
ASTM	American Society for Testing and Materials
C	Cohesion
C_C	Coefficient of curvature
C_c	Compression index
CH	Clay of high plasticity
C_s	Swelling index
C_U	Uniformity coefficient
E	Young's modulus
ES	Expansive soil(s)
FSI	Free swell index
G_s	Specific Gravity
IOT	Iron ore tailing(s)
Is	Shrinkage index
LL	Liquid limit
LOI	Lost on ignition
Ls	Linear shrinkage
MBV	Methylene Blue Value
MDD	Maximum dry density
OMC	Optimum moisture content
PI	Plasticity index
PL	Plastic limit
SEM	Scanning electron microscope
SL	Shrinkage limit
Sp	Swelling pressure
SPLP	Synthetic Precipitation Leaching Procedure
TCLP	Toxicity Characteristic Leaching Procedure
UCS	Unconfined compressive strength
USCS	Unified Soil Classification system
XRD	X-ray diffraction
XRF	X-ray fluorescence
2θ	Angle between transmitted x-ray beam and reflected beam
γ_s	Unit Weight
ρ_d	Dry density
$\sigma'p$	Preconsolidation pressure
$\sigma'v$	Vertical stress
ϕ	Frictional angle

References

Abbey, S.J., Eyo, E.U., & Jeremiah, J.J. (2021). Experimental study on early age characteristics of lime-GGBS-treated gypseous clays under wet-dry cycles. *Geotechnics*, 1(2), 402-415. http://doi.org/10.3390/geotechnics1020019.

Adem, H.H., & Vanapalli, S.K. (2014). Elasticity moduli of expansive soils from dimensional analysis. *Geotechnical Research*, 1(2), 60-72. http://doi.org/10.1680/gr.14.00006.

Adepoju, S.O., & Olaleye, B.M. (2001). Gravity concentration of silica sand from Itakpe iron-ore tailings by tabling operation. *Nigerian Journal of Engineering Management*, 2(2), 51-55.

Ahmadi, H., Satyanaga, A., Orazayeva, S., Kalimuldina, G., Rahardjo, H., Qian, Z., & Kim, J. (2024). Carbon nanotubes for slope stabilization of silty soil. *Infrastructures*, 9(12), 232. http://doi.org/10.3390/infrastructures9120232.

Ajaka, E.O. (2009). Recovering fine iron minerals from Itakpe iron ore process tailing. *Journal of Engineering and Applied Sciences*, 4(9), 17-28.

Aksu, G., & Eskisar, T. (2023). The geomechanical properties of soils treated with nano silica particles. *Journal of Rock Mechanics and Geotechnical Engineering*, 15(4), 954-969. http://doi.org/10.1016/j.jrmge.2022.06.013.

Al-Obaidi, A.L., Yousif, M.A., & Hamid, A.I. (2020). Effect of relative compaction on the bearing capacity of cohesive soils. *IOP Conference Series. Materials Science and Engineering*, 737(1), 012108. http://doi.org/10.1088/1757-899X/737/1/012108.

Altmeyer, W.T. (1955). Discussion of engineering properties of expansive clays. *Proceedings of the American Society of Civil Engineers*, 81(658), 17-19.

ASTM D4943. (2008). *Standard test method for shrinkage factors of soils by the wax method.* ASTM International, West Conshohocken, PA. http://doi.org/10.1520/D4943-08.

ASTM D4546-03. (2010). *Standard test methods for one-dimensional swell or settlement potential of cohesive soils.* ASTM International, West Conshohocken, PA. http://doi.org/10.1520/D4546-03.

ASTM D2435-04. (2011). *Standard test methods for one-dimensional consolidation properties of soils using incremental loading.* ASTM International, West Conshohocken, PA. http://doi.org/10.1520/D2435-04.

ASTM D1632-17. (2017a). *Standard practice for making and curing soil-cement compression and flexure test specimens in the laboratory.* ASTM International, West Conshohocken, PA. http://doi.org/10.1520/D1632-17E01.

ASTM D2166-00. (2017b). *Standard test method for unconfined compressive strength of cohesive soil.* ASTM International, West Conshohocken, PA. http://doi.org/10.1520/D2166-00.

ASTM D2487-17. (2017c). *Standard practice for classification of soils for engineering purposes (unified soil classification system).* ASTM International, West Conshohocken, PA. http://doi.org/10.1520/D2487-06.

ASTM D6528-17. (2017d). *Standard test method for consolidated undrained direct simple shear testing of fine grain soils.* ASTM International, West Conshohocken, PA. http://doi.org/10.1520/D6528-17.

ASTM D4318. (2018). *Standard test methods for liquid limit, plastic limit, and plasticity index of soils.* ASTM International, West Conshohocken, PA. http://doi.org/10.1520/D4318-17E01.

ASTM C618-23. (2019a). *Standard specification for coal fly ash and raw or calcined natural pozzolan for use in concrete.* ASTM International, West Conshohocken, PA. http://doi.org/10.1520/C0618-23E01.

ASTM D4972. (2019b). *Standard test methods for ph of soils.* ASTM International, West Conshohocken, PA. http://doi.org/10.1520/D4972-19.

ASTM C1777. (2020). *Standard test method for rapid determination of the methylene blue value for fine aggregate or mineral filler using a colorimeter.* ASTM International, West Conshohocken, PA. http://doi.org/10.1520/C1777-20.

ASTM D698-12. (2021). *Standard test methods for laboratory compaction characteristics of soil using standard effort (12,400 ft-lb/ft^3 (600 kN-m/m^3))*. ASTM International, West Conshohocken, PA. http://doi.org/10.1520/D0698-12R21.

Benghazi, Z., Tobal, R., & Djellali, A. (2024). Life cycle analysis comparison of stabilizing materials for expansive soils. *ARCHive-SR*, 8(2), 31-37. http://doi.org/10.21625/archive-sr.v8i2.1086.

Blayi, R.A., Omer, B., Sherwani, A.F.H., Hamadamin, R.M., & Muhammed, H.K. (2024). Geotechnical characteristics of fine-grained soil with wood ash. *Cleaner Engineering and Technology*, 18, 100726. http://doi.org/10.1016/j.clet.2024.100726.

Budhu, M. (2011). *Soil mechanics and foundations* (3rd ed.). Hoboken: John Wiley & Sons.

Chassagneux, D., Stieljes, L., Mouroux, P., Ménilliet, F., & Ducreux, G.H. (1996). *Cartographie de l'aléa retrait-gonflement des sols (sécheresse-pluie) à l'échelle départementale: approche méthodologique dans les Alpes de Haute-Provence* (Rapport BRGM, No. R39218,6). Paris (in French).

Chen, F.H. (1988). *Foundations on expansive soils* (Developments in Geotechnical Engineering, No. 12). Amsterdam: Elsevier.

Chethan, L., Nandushree, N., Naveen Kumara, B., & Karthik Kumar, B. (2022). Expansive soil stabilization using iron ore tailings. *International Journal of Advanced Research*, 10, 80-89. http://doi.org/10.21474/IJAR01/15006.

Chu, C., Zhang, F., Wu, D., Zhan, M., & Liu, Y. (2021). Study on mechanical properties of the expansive soil treated with iron tailings sand. *Advances in Civil Engineering*, 2021(1), 9944845. http://doi.org/10.1155/2021/9944845.

Constantinescu, J., & Constantinescu, D. (2011). Particularity of plasticity characteristics of fine glacial materials (north Chicago area). *Geo-Eco-Marina*, 17, 59-66.

Dakshanamurthy, V., & Raman, V. (1973). A simple method of identifying an expansive soil. *Soil and Foundation*, 13(1), 97-104. http://doi.org/10.3208/sandf1972.13.97.

Degirmenci, N., Okucu, A., & Turabi, A. (2007). Application of phosphogypsum in soil stabilisation. *Building and Environment*, 42(9), 3393-3398. http://doi.org/10.1016/j.buildenv.2006.08.010.

Devkota, B., Karim, M.R., Rahman, M.M., & Nguyen, H.B.K. (2022). Accounting for expansive soil movement in geotechnical design: a state-of-the-art review. *Sustainability*, 14(23), 15662. http://doi.org/10.3390/su142315662.

Djellali, A., Sarker, D., Benghazi, Z., & Rais, K. (2022). Geospatial-based approach for susceptibility assessment of expansive soils using a new multicriteria classification model. *Arabian Journal of Geosciences*, 15(23), 1742. http://doi.org/10.1007/s12517-022-11024-2.

Driscoll, R., & Crilly, M. (2000). *Subsidence damage to domestic buildings: Lessons learned and questions asked.* London: Building Research Establishment.

El-Sharkawy, M., Alotaibi, M.O., Li, J., Du, D., & Mahmoud, E. (2025). Heavy metal pollution in coastal environments: ecological implications and management strategies: a review. *Sustainability*, 17(2), 701. http://doi.org/10.3390/su17020701.

Etim, R.K., Attah, I.C., Ekpo, D.U., & Usanga, I.N. (2022). Evaluation on stabilisation role of lime and cement in expansive black clay-oyster shell ash composite. *Transportation Infrastructure Geotechnology*, 9(6), 729-763. http://doi.org/10.1007/s40515-021-00196-1.

Etim, R.K., Eberemu, A.O., & Osinubi, K.J. (2017). Stabilisation of black cotton soil with lime and iron ore tailings admixture. *Transportation Geotechnics*, 10(10), 85-95. http://doi.org/10.1016/j.trgeo.2017.01.002.

Farenzena, H.P., Bruschi, G.J., Medina, G.S., de Sousa Silva, J.P., Lotero, A., & Consoli, N.C. (2024). Iron ore tailings stabilization with alternative alkali-activated cement for dry stacking: mechanical and microstructural insights. *Canadian Geotechnical Journal*, 61(4), 649-667. http://doi.org/10.1139/cgj-2023-0125.

Ferreira, S.R.M., Costa, L.M., Guimarães, L.J.N., & Pontes Filho, I.D.S. (2013). Volume change behavior due to water content variation in an expansive soil from the semiarid region of Pernambuco–Brazil. *Soils and Rocks*, 36(2), 183-193. http://doi.org/10.28927/SR.362183.

Foucault, A., Raoult, J.F., Platevoet, B., & Cecca, F. (2020). *Dictionnaire de géologie: 5000 définitions, plus de 400 shémas et photos en couleurs* (9. ed.). Paris (in French).

Fukue, M., Nakamura, T., & Kato, Y. (1999). Cementation of soils due to calcium carbonate. *Soil and Foundation*, 39(6), 55-64. https://doi.org/10.3208/sandf.39.6_55.

Hossain, K.M.A., & Mol, L. (2011). Some engineering properties of stabilised clayey soils incorporating natural pozzolans and industrial wastes. *Construction & Building Materials*, 25(8), 3495-3501. http://doi.org/10.1016/j.conbuildmat.2011.03.042.

Ibrahim, N.M., Rahim, N.L., Amat, R.C., Salehuddin, S., & Ariffin, N.A. (2012). Determination of plasticity index and compression index of soil at Perlis. *APCBEE Procedia*, 4, 4-98. http://doi.org/10.1016/j.apcbee.2012.11.016.

Ijaz, N., Dai, F., & Ur Rehman, Z. (2020). Paper and wood industry waste as a sustainable solution for environmental vulnerabilities of expansive soil: a novel approach. *Journal of Environmental Management*, 262, 110285. http://doi.org/10.1016/j.jenvman.2020.110285.

Ikeagwuani, C.C. (2021). Estimation of modified expansive soil CBR with multivariate adaptive regression splines, random forest and gradient boosting machine. *Innovative Infrastructure Solutions*, 6(4), 199. http://doi.org/10.1007/s41062-021-00568-z.

Ikeagwuani, C.C., & Nwonu, D.C. (2019). Emerging trends in expansive soil stabilisation: a review. *Journal of Rock Mechanics and Geotechnical Engineering*, 11(2), 423-440. http://doi.org/10.1016/j.jrmge.2018.08.013.

IS 1498. (1987). *Indian Standard classification and identification of soils for general engineering purposes.* Indian Standard, New Delhi.

Jaharou, S. (2015). *Stabilisation of black cotton soil with iron ore tailing* [Doctoral thesis]. Department of Civil Engineering, Faculty of Engineering, University of Ahmadu Bello, Zaria (in Nigeria).

Jayasree, P.K., Balan, K., Peter, L., & Nisha, K.K. (2015). Shrinkage characteristics of expansive soil treated with coir waste. *Indian Geotechnical Journal*, 45(3), 360-367. http://doi.org/10.1007/s40098-015-0144-8.

Ji, X., Xu, Q., Ren, K., Wei, L., & Wang, W. (2025). Compression behavior and particle breakage in iron ore tailings. *Journal of Rock Mechanics and Geotechnical Engineering*, 17(10), 6586-6605. http://doi.org/10.1016/j.jrmge.2025.01.021.

Kaze, C.R., Lecomte-Nana, G.L., Kamseu, E., Camacho, P.S., Yorkshire, A.S., Provis, J.L., Duttine, M., Wattiaux, A., & Melo, U.C. (2021). Mechanical and physical properties of inorganic polymer cement made of iron-rich laterite and lateritic clay: a comparative study. *Cement and Concrete Research*, 140, 106320. http://doi.org/10.1016/j.cemconres.2020.106320.

Khalifa, A.Z., Cizer, Ö., Pontikes, Y., Heath, A., Patureau, P., Bernal, S.A., & Marsh, A.T. (2020). Advances in alkali activation of clay minerals. *Cement and Concrete Research*, 132, 106050. http://doi.org/10.1016/j.cemconres.2020.106050.

Magnan, J.P., & Youssefian, G. (1989). Essai au bleu de méthylène: essai au bleu de méthylène et classification géotechnique des sols. *Bulletin de Liaison des Laboratoires des Ponts et Chaussées*, 159, 93-104.

Moran-Palacios, H., Ortega-Fernandez, F., Lopez-Castaño, R., & Alvarez-Cabal, J.V. (2019). The potential of iron ore tailings as secondary deposits of rare earths. *Applied Sciences*, 9(14), 2913. http://doi.org/10.3390/app9142913.

Nelson, J.D., Chao, K.C., Overton, D.D., & Nelson, E.J. (2015). *Foundation engineering for expansive soils*. Hoboken: John Wiley & Sons.

Ocheme, J.I., Olagunju, S.O., Khamitov, R., Satyanaga, A., Kim, J., & Moon, S.-W. (2023). Triaxial shear behavior of calcium sulfoaluminate (CSA)-treated sand under high confining pressures. *Geomechanics and Engineering*, 33(1), 41-51. http://doi.org/10.12989/gae.2023.33.1.041.

Osinubi, K.J., Yohanna, P., & Eberemu, A.O. (2015). Cement modification of tropical black clay using iron ore tailings as admixture. *Transportation Geotechnics*, 5, 35-49. http://doi.org/10.1016/j.trgeo.2015.10.001.

Paiyz, N., Moon, S.-W., Satyanaga, A., & Kim, J. (2025). Dynamic properties of well-graded sand with silt. *Geomechanics and Engineering*, 41(2), 177-187. http://doi.org/10.12989/gae.2025.41.2.177.

Petit, G., Virollet, M., & Bernard, P. (2013). Swelling quantification of over consolidated soils at excavation base. In *Proceedings of the 18th International Conference on Soil Mechanics and Geotechnical Engineering* (pp. 259-262), Paris. ISSMGE. Retrieved in May 9, 2025, from https://www.cfms-sols.org/actes-du-colloque?lang=en

Plait, R.M. (1953). Determination of swelling pressure of black cotton soil-a method. In *Proceedings of the 3rd International Conference on Soil Mechanics and Foundation Engineering* (Vol. 1, pp. 170-172). ISSMGE.

Québec. Direction du Programme de réduction des rejets industriels et des Lieux contaminés. (2021). *Guide d'intervention - Protection des sols et réhabilitation des terrains contaminés*. Québec: Government of Québec.

Rahaja, N., Kumar Gupta, A., & Kanwar, K. (2024). Enhancing soil stability: the impact of rice husk ash on expansive soil behavior. *E3S Web of Conferences*, 596, 01011. http://doi.org/10.1051/e3sconf/202459601011.

Randhawa, K.S., & Chauhan, R. (2022). Stabilising black cotton soil in subgrade with municipal solid waste incineration ash for lowering greenhouse gas emission: a review. *Materials Today: Proceedings*, 50, 1145-1151. http://doi.org/10.1016/j.matpr.2021.08.037.

Regasa, H., Jothimani, M., & Oyda, Y. (2023). Subgrade soil stabilisation using the Quicklime: a case study from Modjo-Hawassa highway, Central Ethiopia. *International Journal of Geo-Engineering*, 14(1), 17. http://doi.org/10.1186/s40703-023-00197-8.

Roshan, M.J., & Rashid, A.S.B.A. (2024). Geotechnical characteristics of cement stabilised soils from various aspects: a comprehensive review. *Arabian Journal of Geosciences*, 17(1), 1. http://doi.org/10.1007/s12517-023-11796-1.

Sá, T.S.W., Oda, S., Machado, V.K.C.B.L., & Toledo Filho, R.D. (2022). Use of iron ore tailings and sediments on pavement structure. *Construction & Building Materials*, 342, 128072. http://doi.org/10.1016/j.conbuildmat.2022.128072.

Sagidullina, N., Satyanaga, A., Kim, J., & Moon, S.-W. (2025). Engineering behavior and geotechnical challenges of sulfate-rich soils in Astana. *Frontiers in Built Environment*, 10, 1504643. http://doi.org/10.3389/fbuil.2024.1504643.

Sakr, M.A., Azzam, W.R., Meguid, M.A., & Ghoneim, H.A. (2024). Experimental study on the effect of micro-metakaolin on the strength and swelling characteristics of expansive soils. *Arabian Journal for Science and Engineering*, 49(4), 5835-5852. http://doi.org/10.1007/s13369-023-08449-6.

Sambre, T., Endait, M., & Patil, S. (2024). Sustainable soil stabilization of expansive soil subgrades through lime-fly ash admixture. *Discover Civil Engineering*, 1(1), 65. http://doi.org/10.1007/s44290-024-00063-1.

Sani, J.E., Etim, R.K., & Joseph, A. (2019). Compaction behaviour of lateritic soil-calcium chloride mixtures. *Geotechnical and Geological Engineering*, 37(4), 2343-2362. http://doi.org/10.1007/s10706-018-00760-6.

Seed, H.B., Woodward Junior, R.J., & Lundgren, R. (1962). Prediction of swelling potential for compacted clays. *Journal of the Soil Mechanics and Foundations Division*, 88(3), 53-87. http://doi.org/10.1061/JSFEAQ.0000431.

Sharma, L.K., Sirdesai, N.N., Sharma, K.M., & Singh, T.N. (2018). Experimental study to examine the independent roles of lime and cement on the stabilisation of a mountain soil: a comparative study. *Applied Clay Science*, 152, 183-195. http://doi.org/10.1016/j.clay.2017.11.012.

Skempton, A.W. (1953). The colloidal activity of clays. Sel. Pap. *Soil Mechanics*, 1, 57-61.

Spagnoli, G., & Shimobe, S. (2020). An overview on the compaction characteristics of soils by laboratory tests. *Engineering Geology*, 278, 105830. http://doi.org/10.1016/j.enggeo.2020.105830.

Silva, J.P., Carvalho, J.V., Wagner, A.C., & Consoli, N.C. (2024). On the behavior of compacted filtered iron ore tailings submitted to high pressures. *E3S Web of Conferences*, 544, 13004. http://doi.org/10.1051/e3sconf/202454413004.

Tan, Y., Hu, M., & Li, D. (2016). Effects of agglomerate size on California bearing ratio of lime treated lateritic soils. *International Journal of Sustainable Built Environment*, 5(1), 168-175. http://doi.org/10.1016/j.ijsbe.2016.03.002.

Tang, Z., Meng, X., Han, Y., Chen, M., Gao, P., & Zhang, Y. (2024). Hydration and properties of hydrogen-based mineral phase transformation iron ore tailings as supplementary cementitious material. *Journal of Environmental Management*, 356, 120594. http://doi.org/10.1016/j.jenvman.2024.120594.

Tanyildizi, M., Gökalp, İ., Zeybek, A., & Uz, V.E. (2024). Comparative analysis of volume change behavior of expansive road subgrades stabilized with waste paper sludge. *Scientific Reports*, 14(1), 28906. http://doi.org/10.1038/s41598-024-80135-5.

Tong, J., Niu, X., Wang, Y., & Lu, Y. (2021). Strength characteristics of iron tailings blended soil as a road base material. *Applied Sciences*, 11(16), 7587. http://doi.org/10.3390/app11167587.

Turan, C., Javadi, A.A., & Vinai, R. (2022). Effects of class C and class f fly ash on mechanical and microstructural behavior of clay soil-a comparative study. *Materials*, 15(5), 1845. http://doi.org/10.3390/ma15051845.

U.S. Environmental Protection Agency (2024). *Regional Screening Level (RSL) Resident Soil Table*. Washington, D.C.: U.S. EPA.

Vogel, H., & Kasper, B. (2002). *Mine soils on abandoned gold mine tailings in Francistown*. Lobatse: Bundesanstalt für Geowissenschaften und Rohstoffe, Department of Geological Survey (Environmental Geology Division).

Waleed, M., & Alshawmar, F. (2025). Enhancing mechanical properties of low plasticity soil through coal and silica fume stabilization. *Scientific Reports*, 15(1), 9990. http://doi.org/10.1038/s41598-025-94149-0.

Widodo, S., & Ibrahim, A. (2012). Estimation of primary compression index (Cc) using physical properties of Pontianak soft clay. *International Journal of Engineering Research and Applications*, 2(5), 2231-2235.

Wu, J., Liu, L., Deng, Y., Zhang, G., Zhou, A., & Xiao, H. (2022). Use of recycled gypsum in the cement-based stabilisation of very soft clays and its micro-mechanism. *Journal of Rock Mechanics and Geotechnical Engineering*, 14(3), 909-921. http://doi.org/10.1016/j.jrmge.2021.10.002.

Ye, L., Zhu, Q., & Sun, P.P. (2015). Influence of mineral constituents on one-dimensional compression behaviour of clayey soils. *Geotechnical Engineering*, 46(3), hal-01472596.

Yu, H., Huang, X., Ning, J., Zhu, B., & Cheng, Y. (2014). Effect of cation exchange capacity of soil on stabilised soil strength. *Soil and Foundation*, 54(6), 1236-1240. http://doi.org/10.1016/j.sandf.2014.11.016.

Yukselen, Y., & Kaya, A. (2008). Suitability of the methylene blue test for surface area, cation exchange capacity and swell potential determination of clayey soils. *Engineering Geology*, 102(1-2), 38-45. http://doi.org/10.1016/j.enggeo.2008.07.002.

Zeghichi, L., & Benghazi, Z. (2011). Physical effects of natural pozzolana on alkali-activated slag cement. *World Journal of Engineering*, 8(2), 141-146. http://doi.org/10.1260/1708-5284.8.2.141.

Zereg, S., Boudoukha, A., & Benaabidate, L. (2018). Impacts of natural conditions and anthropogenic activities on groundwater quality in Tebessa plain, Algeria. *Sustainable Environment Research*, 28(6), 340-349. http://doi.org/10.1016/j.serj.2018.05.003.

Zimar, Z., Robert, D., Zhou, A., Giustozzi, F., Setunge, S., & Kodikara, J. (2022). Application of coal fly ash in pavement subgrade stabilisation: a review. *Journal of Environmental Management*, 312, 114926. http://doi.org/10.1016/j.jenvman.2022.114926.

Zimar, Z., Robert, D., Giustozzi, F., Zhou, A., Setunge, S., & Kodikara, J. (2024). Use of industrial wastes for stabilizing expansive clays in pavement applications: durability and microlevel investigation. *Acta Geotechnica*, 19(9), 6259-6287. http://doi.org/10.1007/s11440-024-02298-9.